

Linear Thermal Expansion Coefficient of Silicon from 293 to 1000 K

Hirromichi Watanabe,^{1,2} Naofumi Yamada,¹ and Masahiro Okaji^{1,3}

Received September 2, 2003

As a part of the program to establish a thermal expansion standard, the linear thermal expansion coefficients of single-crystal silicon have been determined in the temperature range 293 to 1000 K using a dilatometer which consists of a heterodyne laser Michelson interferometer and gold versus platinum thermocouple. The relative standard deviation of the measured values from those calculated from the best least-squares fit was 0.21%. The relative expanded uncertainty in the measurement was estimated to be 1.1 to 1.5% in the temperature range, based upon an analysis of thirteen standard uncertainties. The present data are compared with the data previously obtained by similar dilatometers and the standard reference data for the thermal expansion coefficient of silicon, recommended by the Committee on Data for Science and Technology (CODATA). The present data are in good agreement with the most recently reported data but not with the earlier high-temperature data used to evaluate the standard reference data, which suggests a need for the reevaluation of the standard reference data for the thermal expansion coefficient of silicon at temperatures above 600 K.

KEY WORDS: gold versus platinum thermocouple; heterodyne interferometer; reference material; silicon; standard reference data; thermal expansion.

1. INTRODUCTION

Silicon is an ideal reference material for thermal expansion measurements, because it is isotropic in thermal expansion owing to its diamond-like crystallographic structure and because it is readily available in an ultra-pure

¹ Thermophysical Properties Section, National Metrology Institute of Japan, AIST, 1-1-1 Umezono, Tsukuba, Ibaraki 305-8563, Japan.

² To whom correspondence should be addressed. E-mail: hirromichi-watanabe@aist.go.jp

³ International Affairs Department, AIST, 1-1-1 Umezono, Tsukuba, Ibaraki 305-8563, Japan.

condition as a result of the needs of the electronics industries. During the 1970s, cooperative measurements made by various laboratories indicated that the linear thermal expansion coefficients, $\alpha(T)$, for various samples of semi-conductor grade, polycrystalline, and single-crystal silicon agreed within $0.01 \times 10^{-6} \text{ K}^{-1}$ in the temperature range 280 to 420 K [1]. In 1983, therefore, Swenson made a critical evaluation of previously reported $\alpha(T)$ for silicon and produced “recommended values” of $\alpha(T)$ as a function of temperature T for the CODATA Task Group on Thermophysical Properties [2]. The CODATA recommended values were deduced from various absolute determinations of $\alpha(T)$ for both single-crystal and polycrystalline silicon at temperatures below 850 K, and thus the recommended values were limited to the temperature range 90 to 850 K. In 1988, Okaji [3] reported absolute measurements of $\alpha(T)$ on single-crystal silicon at temperatures up to 1300 K using a laser interferometric dilatometer (LID 1). The feature of LID 1 was a heterodyne laser Michelson interferometer [4], which results in excellent resolution and accuracy for the measurement of the length change. Swenson has included the data measured with LID 1 in a reevaluation [1] of the CODATA recommended values of $\alpha(T)$ for silicon for the temperature range 90 to 1300 K.

Recently, we have made refinements and improvements to most parts of LID 1 and have determined $\alpha(T)$ of silicon using the modified dilatometer (LID 2) [5]. Comparison of $\alpha(T)$ measured with LID 1 and LID 2 for the same silicon sample reveals that values of $\alpha(T)$ measured with LID 1 in the temperature range 700 to 1100 K are systematically smaller than those with LID 2. The disagreement suggests that the measured data for LID 1 in this temperature range include some systematic errors, which can be reduced in the measurement with LID 2. Accordingly, there is concern about the reliability of the standard reference data for $\alpha(T)$ of silicon, because the present CODATA recommended values at temperatures above 800 K were mainly attributed to the data measured with LID 1.

Despite the effective improvements, data of $\alpha(T)$ measured with LID 2 are insufficient for the standard reference data, because of several experimental shortcomings that may lead to serious systematic errors in the temperature measurement below 700 K. In the previous work, a high-temperature platinum resistance thermometer (HTPRT) was used to measure the sample temperature and the furnace was evacuated to 10^{-3} Pa . The reduced heat transfer due to the absence of gas makes the thermal contact between the sample and HTPRT become worse at lower temperatures. The importance of the presence of thermal exchange gas at an appropriate pressure has been pointed out in ASTM E 289 “Standard Test Method for Linear Thermal Expansion of Rigid Solids with Interferometry.” In

addition, there was a possibility that the HTPRT was so long (30 mm in length) that sufficient temperature uniformity within the sensor could not be attained. As a result, we could not determine $\alpha(T)$ of silicon below 700 K using LID 2, and the absence of the data below 700 K influences the reliability of our previous data measured using LID 2.

The objective of the present work is to determine reliable data for linear thermal expansion coefficients of silicon in the temperature range 293 to 1000 K. This work is a part of a project to establish reference materials for measurements of thermal expansion of solids. To reduce the temperature difference between the sample and thermometer, the measurements were undertaken with the sample in helium at an appropriate pressure. The temperature measurements were corrected for the residual temperature difference between the sample and thermometer. The sample temperatures were measured using an elemental thermocouple of which the achievable accuracy was comparable to that of the HTPRT to avoid the possible error associated with the size of the thermometer sensor. In addition, a detailed evaluation of experimental uncertainty was carried out.

2. EXPERIMENTAL

The present interferometric dilatometer (LID 3) was almost the same as LID 2 [5]. Therefore, we describe here an outline of the measurements and differences from the operations of LID 2.

In the present work, values of $\alpha(T)$ were calculated by applying

$$\alpha(T) = \Delta L / (L_0 \Delta T), \quad (1)$$

where ΔT is a given temperature change from T_n to T_{n+1} , T is $(T_n + T_{n+1})/2$, L_0 is the initial length of the sample at room temperature, T_0 (293 K), and ΔL is the change of sample length from $L(T_n)$ to $L(T_{n+1})$. We present here the linear thermal expansion, $e(T)$, calculated using the following expression in regard to the practical availability of thermal expansion data,

$$e(T) = (L(T) - L_0) / L_0. \quad (2)$$

Values of ΔL , ΔT , and L_0 were measured with a heterodyne laser Michelson interferometer, a gold versus platinum (Au/Pt) thermocouple, and a linear gauge, respectively. Details of the optical system of the interferometer are described in our previous papers [5–7]. The interferometer employed a double-path system so that

$$\Delta L = \frac{\lambda}{4} \left(\frac{\Delta \theta_p}{2\pi} \right), \quad (3)$$

where λ is the wavelength of laser in the furnace and $\Delta\theta_p$ is the difference in the phase of the beat signal for optical heterodyne interferometry measured on changing the temperature from T_n to T_{n+1} .

Two samples of single-crystal silicon in which the crystallographic axes are oriented in [100] and [110] directions were prepared from an ingot made using a floating-zone method, which is the same batch as that investigated in our previous works [3, 5]. Each sample was in the form of a perpendicular block whose size was 10 mm \times 7 mm \times 20 mm. The (7 \times 20) surfaces were polished to be flat to within one tenth of a wavelength of 632.8 nm and parallel within 5 arc s. The sample was placed on the flat base plate, which was also made of single-crystal silicon. The mirror face of the base plate was polished as was that of the sample. A hole having a diameter of 4 mm was bored down the symmetry axis through the optical flats of the sample and the base plate.

The Au/Pt thermocouple consisted of gold and platinum wires having a diameter of 0.25 mm and an insulation tube made of alumina. The thermocouple was encased in a fused-quartz tube of 3 mm in diameter, and it was inserted into the hole of the sample. The equation used to compute the temperature was deduced from the standard reference function given in ASTM E 1751, the thermocouple calibration at the metal freezing points of zinc, aluminum, and silver, and the correction for the temperature difference (Δ_s) between the sample (T_{true}) and the thermocouple (T_{exp}). Δ_s as a function of temperature was experimentally estimated using a "dummy" silicon sample with a differential thermocouple consisting of two platinum and one platinum-13 mass% rhodium alloy wires, and a type R thermocouple in a mineral-insulated, metal-sheathed (MIMS) configuration. Figure 1 shows a schematic diagram of the arrangement of the dummy sample and thermocouples to measure Δ_s and T . The dummy sample had two extra holes into which the MIMS thermocouples were inserted. To attain good thermal contact, the diameter of the holes was made almost the same as that of the metal sheath (1.6 mm). The following correction function was given by four repeated measurements of Δ_s in the temperature range 293 to 1100 K:

$$\Delta_s(T) = -0.070 + 0.00108(T - 293), \quad (4)$$

which was used to compensate for Δ_s in the measurements of $\alpha(T)$.

The measurements of $\alpha(T)$ were made while the sample was heated or cooled successively to constant temperatures between which there were temperature intervals of approximately 50 or 25 K. In order to improve thermal contact between the sample and thermocouple, an amount of helium gas at a pressure of 80 Pa and a temperature of 293 K was sealed in the furnace. After one measurement cycle of heating to approximately

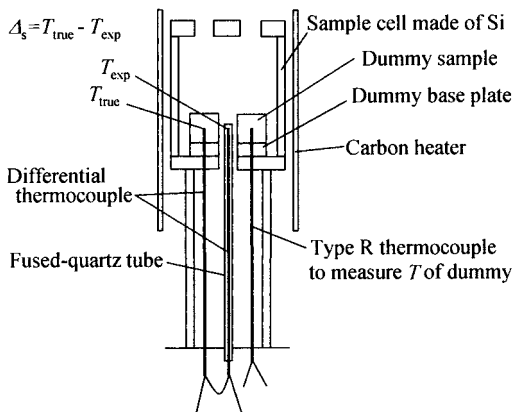


Fig. 1. Schematic diagram of the arrangement of the sample and differential thermocouple.

1050 K and then cooling to 293 K, the gas pressure at 293 K increased by about 30 Pa as a result of gas evolution from the furnace wall. Taking into account the gas evolution resulting in the pressure increase from 80 to 110 Pa, we considered the average amount of helium gas during the experiment to be that at a pressure of 95 Pa and a temperature of 293 K. Thus, the value of λ was calculated to be 632.991 nm using the refractive index of helium gas at 95 Pa and 293 K. The temperature of the sample changed at a rate of less than $1.7 \times 10^{-2} \text{ K} \cdot \text{s}^{-1}$ from one constant temperature to the next one. The temperature was kept at each of the temperature steps for a time period longer than $3.6 \times 10^3 \text{ s}$ to attain thermal equilibrium. The optical window of the furnace was in contact with a brass plate whose temperature was kept constant using two thermoelectric transducers in order to reduce the uncertainty due to the temperature distribution within the window through which the laser beams pass.

3. RESULTS

Figure 2 shows the experimental results for $\alpha(T)$ for the two silicon samples. For each sample, the measurement in the temperature range 293 to 1025 K was repeated six times; three runs were carried out during heating and cooling, respectively. All of the data were pooled, and the following fifth-order polynomial function of temperature was obtained by the method of least squares: at $293 \leq T \leq 1025$

$$\begin{aligned} \alpha(T)/(10^{-6} \text{ K}^{-1}) = & -3.0451 + 0.035705T - 7.981 \times 10^{-5}T^2 \\ & + 9.5783 \times 10^{-8}T^3 - 5.8919 \times 10^{-11}T^4 \\ & + 1.4614 \times 10^{-14}T^5. \end{aligned} \quad (5)$$

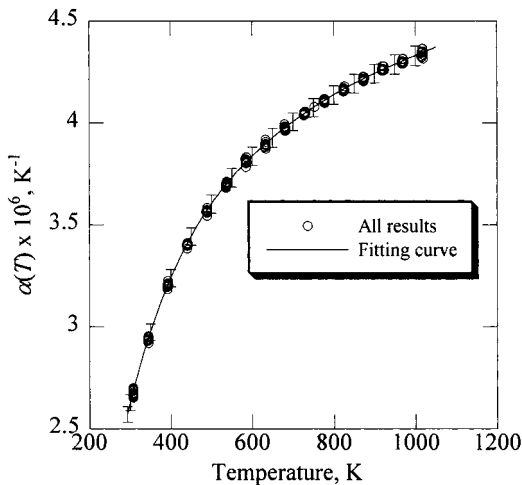


Fig. 2. Linear thermal expansion coefficient, $\alpha(T)$, of silicon as a function of temperature.

The polynomial function is shown as a solid line in Fig. 2. The standard deviation of this fit with 192 data points and its relative value is $7.5 \times 10^{-9} \text{ K}^{-1}$ and 0.21%, respectively. The error bar attached to the line illustrates the expanded uncertainty ($k = 2$), an estimation of which will be described in Section 4.1. Figure 3 shows the difference of the data points from $\alpha(T)$ calculated using Eq. (5). The unfilled and filled circles and triangles shown in Fig. 3 correspond to $\alpha(T)$ obtained during heating and cooling for the [100] and [110] samples, respectively. Inspection of Fig. 3 indicates that there was no appreciable deviation between values of $\alpha(T)$ for the two samples but that values of $\alpha(T)$ measured (ca. 1000 K) during heating at the upper limit of the temperature were systematically larger than those measured during cooling.

Table I gives the data of $\alpha(T)$ and $e(T)$ calculated from the fitting functions and their expanded uncertainties. The values of $e(T)$ listed in the table were calculated from the following equation based upon a least-squares analysis of the experimental data of $e(T)$ from the two samples: at $300 \leq T \leq 1025$

$$e(T) \times 10^6 = -426.68 - 0.090926T + 0.0065359T^2 - 4.7219 \times 10^{-6}T^3 + 1.3822 \times 10^{-9}T^4. \quad (6)$$

The standard deviation of this fit is 1.1×10^{-6} with 204 data points.

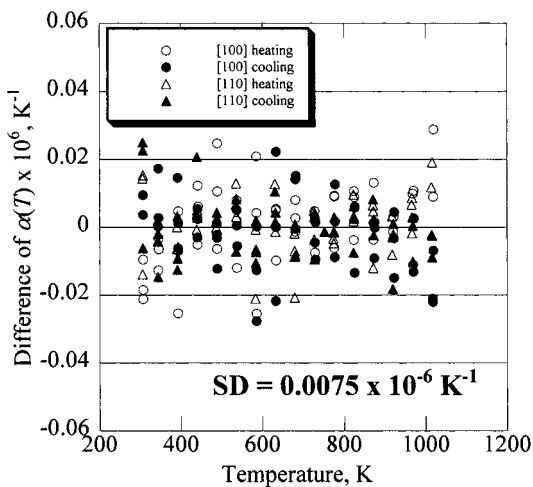


Fig. 3. Differences of the present results for $\alpha(T)$ from the best least-squares fit.

Table I. Results of Thermal Expansion Measurements and Expanded Uncertainties for Silicon in Temperature Range 293 to 1000 K

Temperature T (K)	Linear thermal expansion $e(T) \times 10^6$	Expanded uncertainty ($k=2$) $\delta e(T) \times 10^6$	Linear thermal expansion coefficient $\alpha(T) \times 10^6$ (K^{-1})	Expanded uncertainty ($k=2$) $\delta \alpha(T) \times 10^6$ (K^{-1})
293	0	null	2.57	0.038
300	18.0	1.6	2.63	0.039
350	160.4	1.7	2.97	0.040
400	315.9	1.9	3.24	0.042
450	482.3	2.2	3.44	0.043
500	658.0	2.6	3.60	0.045
550	841.3	2.9	3.73	0.045
600	1031	3.3	3.84	0.046
650	1226	3.7	3.93	0.047
700	1425	4.1	4.00	0.044
750	1627	4.5	4.07	0.045
800	1832	5.0	4.14	0.045
850	2040	5.4	4.19	0.046
900	2250	5.8	4.24	0.046
950	2463	6.3	4.29	0.048
1000	2679	6.7	4.33	0.048

4. DISCUSSION

4.1. Estimates of Uncertainties

4.1.1. Outline of Estimates

Tables II and III give the respective uncertainty budgets of the linear thermal expansion coefficient (α) and linear thermal expansion (e) for silicon measured at 1000 K. The relative combined standard uncertainty ($\delta\alpha/\alpha$) listed in Table II is calculated using

$$\delta\alpha/\alpha = \sqrt{\sum \{\delta(\Delta L)/\Delta L\}^2 + \sum \{\delta(\Delta T)/\Delta T\}^2 + \sum (\delta L_0/L_0)^2} \quad (7)$$

where $\delta(\Delta L)$, $\delta(\Delta T)$, and δL_0 are the standard uncertainties of ΔL , ΔT , and L_0 , respectively. The magnitudes of uncertainties in Table II were estimated under the measurement conditions that ΔT was 50 K, L_0 was 10 mm, α was calculated from Eq. (5) at 1000 K, and ΔL was given by

$$\Delta L = \alpha L_0 \Delta T. \quad (8)$$

On the other hand, the relative combined standard uncertainty ($\delta e/e$) listed in Table III is calculated by using

$$\delta e/e = \sqrt{\sum \{\delta(\Delta L)/\Delta L\}^2 + \sum (\alpha \delta T/e)^2 + \sum (\delta L_0/L_0)^2} \quad (9)$$

where δT is the standard uncertainty of the temperature. The second term in the square root of Eq. (9) accounts for the strong dependence of e on temperature. In the estimation of $\delta e/e$, the value of e was calculated from Eq. (6), L_0 was 10 mm, and ΔL was given by

$$\Delta L = e L_0. \quad (10)$$

In both the uncertainty estimations we attempted to address the standard uncertainties corresponding to the thirteen original uncertainties listed in the two tables. The original uncertainties are divided into three categories, as described below.

4.1.2. Uncertainties Associated with Measurements of Length Change

The first and second uncertainties listed are due to the uncertainty ($\delta\lambda$) of the wavelength of the laser in the furnace. The wavelength was calibrated by a beat frequency comparison to an iodine stabilized reference laser. The beat frequency comparison was carried out over 720 minutes at a data acquisition rate of six points per minute. The calibration uncertainty

Table II. Uncertainty Budget of Linear Thermal Expansion Coefficient, α , for Silicon at 1000 K

Measurement conditions						
T (K)	ΔT (K)	L_0 (m)	α (K ⁻¹)	ΔL (m) ^a		
1000	50	1.0×10^{-2}	4.33×10^{-6}	2.16×10^{-6}		
Uncertainty source	Type	Original uncertainty	Probability distribution	Divisor	Relative uncertainty (%)	Uncertainty
Terms associated with ΔL		$\delta\lambda$ (m)		d	$\delta(\Delta L)/\Delta L$	
1. Calibration uncertainty of laser wavelength	A	2.53×10^{-16}	normal	1	3.99×10^{-8}	
2. Instability of refraction index of gas	A	3.32×10^{-15}	normal	1	5.25×10^{-7}	
		$\delta\theta_m$ (rad)				
3. Nonparallelism of the sample top surface and the base plate	B	1.88×10^{-3}	rectangular	1.73	1.03×10^{-4}	
		$\delta\theta_p$ (rad)				
4. Uncertainty of measurement of phase with lock-in amplifier	B	1.75×10^{-2}	rectangular	1.73	1.66×10^{-2}	
		$\delta(\Delta L)$ (m)				
5. Temperature distribution within optical components	A	4.68×10^{-9}	normal	1	2.87×10^{-1}	
Terms associated with ΔT		δT (K)			$\delta(\Delta T)/\Delta T$	
6. Calibration uncertainty of thermocouple	B	3.03×10^{-1}	normal	2	4.28×10^{-1}	
7. Uncertainty of correction for temperature difference between sample and thermocouple	A	5.81×10^{-2}	normal	1	1.64×10^{-1}	
8. Instability of ice point	B	2.00×10^{-2}	rectangular	1.73	3.27×10^{-2}	
		δV_{emf} (mV)				
9. Uncertainty of measurement of emf with DMM	B	1.60×10^{-3}	rectangular	1.73	1.23×10^{-1}	
Terms associated with L_0		δL_0 (m)			$\delta L_0/L_0$	
10. Uncertainty in reading of linear gauge	B	4.00×10^{-8}	normal	2	2.00×10^{-4}	
11. Nonparallelism of sample	A	3.17×10^{-8}	normal	1	3.17×10^{-4}	
12. Temperature difference from T_0	B	1.73×10^{-7}	rectangular	1.73	1.00×10^{-3}	
13. Resolution of linear gauge	B	5.00×10^{-7}	rectangular	1.73	2.89×10^{-3}	
Combined standard uncertainty					$\delta\alpha/\alpha^b$	
Expanded uncertainty ($k = 2$)					0.556	2.41×10^{-8}
					1.11	4.82×10^{-8}

^a $\Delta L = \alpha L_0 \Delta T$.

^b $\delta\alpha/\alpha = \sqrt{\sum \{\delta(\Delta L)/\Delta L\}^2 + \sum \{\delta(\Delta T)/\Delta T\}^2 + \sum (\delta L_0/L_0)^2}$.

Table III. Uncertainty Budget of Linear Thermal Expansion, e , for Silicon at 1000 K

Measurement conditions						
T (K)	T_0 (K)	L_0 (m)	e	ΔL (m) ^a	α (K ⁻¹)	
1000	293	1.0×10^{-2}	2.679×10^{-3}	2.679×10^{-5}	4.33×10^{-6}	
Uncertainty source	Type	Original uncertainty	Probability distribution	Divisor	Relative uncertainty (%)	Uncertainty
Terms associated with ΔL		$\delta\lambda$ (m)		d	$\delta(\Delta L)/\Delta L$	
1. Calibration uncertainty of laser wavelength	A	2.53×10^{-16}	normal	1	3.99×10^{-8}	
2. Instability of refraction index of gas	A	3.32×10^{-15}	normal	1	5.25×10^{-7}	
3. Nonparallelism of the sample top surface and the base plate		$\delta\theta_m$ (rad)				
	B	1.88×10^{-3}	rectangular	1.73	1.03×10^{-4}	
4. Uncertainty of measurement of phase with lock-in amplifier		$\delta\theta_p$ (rad)				
	B	1.75×10^{-2}	rectangular	1.73	1.34×10^{-3}	
5. Temperature distribution within optical components		$\delta(\Delta L)$ (m)				
	A	3.26×10^{-8}	normal	1	1.23×10^{-1}	
Terms associated with T		δT (K)			$\alpha \delta T/e$	
6. Calibration uncertainty of thermocouple	B	3.03×10^{-1}	normal	2	2.45×10^{-2}	
7. Uncertainty of correction for temperature difference between sample and thermocouple	A	5.81×10^{-2}	normal	1	9.39×10^{-3}	
8. Instability of ice point	B	2.00×10^{-2}	rectangular	1.73	1.87×10^{-3}	
9. Uncertainty of measurement of emf with DMM		δV_{emf} (mV)				
	B	1.60×10^{-3}	rectangular	1.73	7.03×10^{-3}	
Terms associated with L_0		δL_0 (m)			$\delta L_0/L_0$	
10. Uncertainty in reading of linear gauge	B	4.00×10^{-8}	normal	2	2.00×10^{-4}	
11. Nonparallelism of sample	A	3.17×10^{-8}	normal	1	3.17×10^{-4}	
12. Temperature difference from T_0	B	2.19×10^{-7}	rectangular	1.73	1.26×10^{-3}	
13. Resolution of linear gauge	B	5.00×10^{-7}	rectangular	1.73	2.89×10^{-3}	
Combined standard uncertainty					$\delta e/e^b$	
Expanded uncertainty ($k = 2$)						
					0.126	3.37×10^{-6}
					0.252	6.75×10^{-6}

^a $\Delta L = L - L_0 = eL_0$.^b $\delta e/e = \sqrt{\sum \{\delta(\Delta L)/\Delta L\}^2 + \sum (\alpha \delta T/e)^2 + \sum (\delta L_0/L_0)^2}$.

of the wavelength was estimated to be 2.53×10^{-16} m, which was the standard deviation of the measured wavelengths from the mean. The instability of the refraction index of the helium gas in the furnace was caused by the gas evolution from the inside wall of the furnace. The standard uncertainty of the laser wavelength due to the change in the refraction index was estimated to be 3.32×10^{-15} m from the observed pressure change from 80 to 110 Pa after one cycle of heating and cooling. The relative uncertainties due to the first and second sources are calculated as follows:

$$\delta(\Delta L)/\Delta L = \delta\lambda/(\lambda d), \quad (11)$$

where d is the divisor determined from the probability distribution and coverage factor of the original uncertainty.

The third uncertainty is attributed to a possible nonparallelism of the sample top surface and the base plate. For the double-path Michelson interferometer, the relative standard uncertainty caused by the tilt of the sample top surface to the base plate is roughly estimated as follows:

$$\delta(\Delta L)/\Delta L = -\delta\theta_m^2/(2d), \quad (12)$$

where $\delta\theta_m$ is the tilt angle between the sample top surface and the base plate in radians. The double-path interferometer considerably reduces the requirement of the parallelism, because the incident and reflected laser beams are maintained mutually parallel even in the case where there is tilt of the optical system or nonparallelism between the top and bottom surfaces of the sample [8]. However, the value of $\delta\theta_m$ in the present work was limited to 1.88×10^{-3} rad (0.108 deg) based upon the following inequality:

$$2l \tan(2\delta\theta) \leq (D_{LB} + D_{PD})/2, \quad (13)$$

where l was the distance (600 mm) between the sample and the cube corner prism used to return the laser beams to the sample, D_{LB} was the diameter (3 mm) of the laser beams, and D_{PD} was the diameter (6 mm) of the circular sensing area of the photodetector. The left side of the inequality equals the distance by which the nonparallelism of $\delta\theta_m$ makes the reflected beam shift from parallel. The interference signal dissipates if the distance becomes greater than that given by the right side of the inequality. Therefore, the relative uncertainty due to the third source was calculated by substituting the upper limit of $\delta\theta_m$ into Eq. (12) on the assumption that the probability distribution was a rectangular one.

The fourth uncertainty is associated with the uncertainty of the measurement of the phase (θ_p) of the beat signal with the lock-in amplifier used

in the present work. The magnitude of the fourth original uncertainty ($\delta\theta_p$) was reported as 1.75×10^{-2} rad (1 degree) from the manufacturer of the lock-in amplifier (SRS, Model SR830). The phase shift ($\Delta\theta_p$) corresponding to ΔL is obtained by the two determinations of θ_p , and thus $\delta\theta_p$ multiplied by $\sqrt{2}$ equals the uncertainty of $\Delta\theta_p$. Therefore, the relative uncertainty is calculated using

$$\frac{\delta(\Delta L)}{\Delta L} = \frac{\sqrt{2} \lambda}{d \Delta L 4} \left(\frac{\delta\theta_p}{2\pi} \right). \quad (14)$$

The fifth uncertainty is associated with the temperature distribution within optical components through which the laser beams pass. It is impossible to eliminate temperature distributions within all the optics that are irradiated by the thermal radiation from the furnace. The residual temperature distribution causes a difference in refractive index within the optics, which leads to the apparent length change [9]. Figure 4 shows a typical experimental result of the apparent length change for the case where only the base plate was subjected to the same stepwise heating cycle as that carried out in the thermal expansion measurement. The filled circles and error bars correspond to the mean value and the fluctuation of the apparent length change while the temperature of the plate was held constant, respectively. The slope of the line between the two circles is referred to as the zero drift. The apparent length measurement from 293 to 1050 K

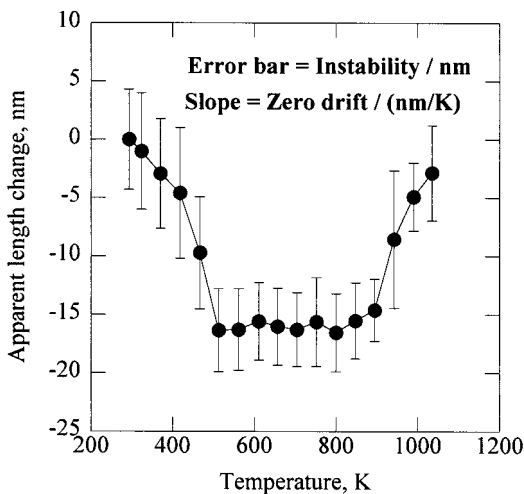


Fig. 4. Typical change in apparent length in the case where only the base plate was set in the furnace.

was repeated two times during heating and cooling. The value of the original uncertainty was calculated as follows:

$$\delta(\Delta L) = \sqrt{(\sqrt{2} \delta L_A)^2 + (\Delta T \cdot S_A)^2}, \quad (15)$$

where δL_A and S_A were the respective average values of the instability and the magnitude of the zero drift obtained during the four measurement runs.

4.1.3. Uncertainties Associated with Temperature Measurements

First, it should be noted that the temperature uncertainty (δT) multiplied by $\sqrt{2}$ equals the uncertainty of ΔT , because ΔT is obtained from the two determinations of T . The sixth original uncertainty is identical to the expanded uncertainty ($k = 2$) associated with the thermocouple calibration at the three metal freezing points, the value of which was provided from the calibration laboratory (Yamari Industries) of the thermocouple. The value of the seventh original uncertainty was estimated as the standard deviation of the measured Δ_s from the correction function given by Eq. (4). The eighth uncertainty is associated with the fluctuation of the temperature of the cold junction of the thermocouple. The temperature of the junction was stabilized by an automatic ice-point cell. The long-term instability of the ice point realized by the cell was used to estimate the eighth uncertainty. The ninth uncertainty is associated with the uncertainty of the measurement of the voltage (V_{emf}) of the thermocouple emf with a digital multimeter (DMM) used in the present work. The magnitude of the ninth original uncertainty (δV_{emf}) was calculated using the relation between the dc voltage reading and accuracy, which was provided from the manufacturer of the DMM (Keithley, Model 2001).

4.1.4. Uncertainties Associated with Measurements of Initial Length of Sample

The tenth original uncertainty is identical to the expanded uncertainty ($k = 2$) of the length of the gauge block used for the correction of the reading of the linear gauge carried out before and after the measurement of L_0 . The value of the expanded uncertainty was provided from the manufacturer (Mitsutoyo) of the gauge block. The eleventh original uncertainty is estimated from the nonparallelism of the top and bottom surfaces of the sample. The twelfth uncertainty is associated with the possible temperature difference between T_0 and the real temperature on the measurements of L_0 . The listed value of the twelfth original uncertainty was estimated from the thermal expansion or contraction due to the expected maximum temperature difference (2 K) on the assumption that the probability distribution was a rectangular one. The last original uncertainty is

identical to the uncertainty due to the resolution of the linear gauge (Sony, Model DZ521).

4.2. Comparisons with Previously Reported Data

Figure 5 shows four sets of the differences from the present results (Eq. (5)) for the data previously measured with LID 1 and LID 2 and the previous and present CODATA recommended data (CODATA 1 and CODATA 2). The thick solid and broken lines correspond to the data for LID 1 and LID 2, and the unfilled and filled circles indicate the CODATA 1 and CODATA 2, respectively. Two thin broken lines denote the positive and negative expanded uncertainties in the present measurements.

It must be emphasized that the present results are in good agreement with the data measured using LID 2 but not with those measured using LID 1 in a temperature range 700 to 1000 K. From the characteristics of LID 1, we can consider that the earlier high-temperature data included systematic errors due to the following factors: (a) temperature difference between sample and thermocouple, (b) long-term drift in the signal of the thermocouple, and (c) the periodic nonlinearity due to imperfect separation of the two optical frequencies. In the operation of LID 1, the sample was rapidly heated with a radiant image furnace and a type R thermocouple was used to measure the sample temperature. In general, it is difficult to

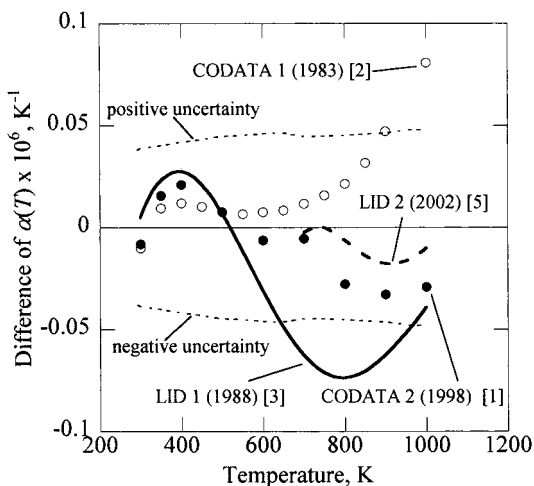


Fig. 5. Differences of $\alpha(T)$ measured with LID 1 and LID 2 and the present and previous CODATA recommended data from the present results.

uniformly heat the bulk sample and thermometer using radiant image furnaces. A fairly large temperature difference between the sample and thermometer or a serious nonuniformity in temperature within the sample would exist in the measurement. Compared to the Au/Pt thermocouple and HTPRT, type R thermocouples are sufficiently sensitive but lack long-term stability. It is considered that the use of a Zeeman laser as the light source of the heterodyne interferometry in LID 1 increased the periodic nonlinearity, more or less. In the operations of the later interferometers (LIDs 2 and 3), the probe and reference laser beams were generated using the combination of a stabilized He-Ne laser unit and a pair of acousto-optical modulators to reduce the periodic nonlinearity. From the concerns about the significant error, we can conclude that the standard reference data should be reevaluated without the data measured using LID 1 at temperatures above 600 K, although the difference between the present data and CODATA 2 is within the magnitude of the expanded uncertainty in the present work.

5. CONCLUSIONS

Linear thermal expansion data, $\alpha(T)$ and $e(T)$, on single-crystal silicon in the temperature range 293 to 1000 K have been determined using a laser interferometric dilatometer. The expanded uncertainties ($k=2$) of $\alpha(T)$ and $e(T)$ in the measured temperature range were estimated to be 3.8×10^{-8} to $4.8 \times 10^{-8} \text{ K}^{-1}$ and 1.6×10^{-6} to 6.7×10^{-6} , respectively. The respective standard deviations of the measured $\alpha(T)$ and $e(T)$ were estimated to be $7.5 \times 10^{-9} \text{ K}^{-1}$ and 1.1×10^{-6} , which were within the magnitudes of their expanded uncertainties.

The present results are in good agreement with the most recently reported data [5] but not with the earlier reported data at temperatures above 700 K [3], both of which were measured with the dilatometers similar to that used in the present work. The poor agreement with the earlier reported data, which were used to estimate the present CODATA recommended values [1], suggests the need for a reevaluation of the standard reference values of $\alpha(T)$ on silicon at temperatures above 600 K.

ACKNOWLEDGMENTS

The authors wish to thank Dr. Jun Ishikawa of the Time and Frequency Division of our institute, who calibrated the wavelength of the laser used in this work. This work is a result of the national research program "Research on Measurement Technology and Reference Materials for Thermophysical Properties of Solids" which was financially supported

by the Promotion System for Intellectual Infrastructure of Research and Development.

REFERENCES

1. G. K. White, in *CINDAS Data Series on Material Properties, Vols. 1–4: Thermal Expansion of Solids*, R. E. Taylor, ed. (ASM International, Materials Park, OH, 1998), Chap. 11, pp. 269–285.
2. C. A. Swenson, *J. Phys. Chem. Ref. Data* **12**:179 (1983).
3. M. Okaji, *Int. J. Thermophys.* **9**:1101 (1988).
4. M. Tanaka, T. Yamagami, and K. Nakayama, *IEEE Trans. Instrum. Meas.* **38**:552 (1989).
5. H. Watanabe, N. Yamada, and M. Okaji, *Int. J. Thermophys.* **23**:543 (2002).
6. N. Yamada and M. Okaji, *High Temp. High Press.* **29**:89 (1997).
7. H. Watanabe, N. Yamada, and M. Okaji, *Int. J. Thermophys.* **22**:1185 (2001).
8. M. Okaji and H. Imai, *Prec. Eng.* **7**:206 (1985).
9. M. Okaji and H. Imai, *J. Phys. E* **20**:887 (1987).